Bone Reports 15 (2021) 101140

Contents lists available at ScienceDirect

Bone Reports

journal homepage: www.elsevier.com/locate/bonr

Genetic variability affects the skeletal response to immobilization in founder strains of the diversity outbred mouse population

Michael A. Friedman [a], Abdullah Abood [b], Bhavya Senwar [c], Yue Zhang [a], Camilla Reina Maroni [a,d], Virginia L. Ferguson [c], Charles R. Farber [b], Henry J. Donahue [a,*]

[a] Virginia Commonwealth University, Richmond, VA 23284, USA
[b] University of Virginia, Charlottesville, VA 22908, USA
[c] University of Colorado, Boulder, CO 80309, USA
[d] D'Annunzio University of Chieti-Pescara, Chieti, Italy

ARTICLE INFO

Keywords:
Genetic variability
Immobilization
Heritability
Bone loss

ABSTRACT

Mechanical unloading decreases bone volume and strength. In humans and mice, bone mineral density is highly heritable, and in mice the response to changes in loading varies with genetic background. Thus, genetic variability may affect the response of bone to unloading. As a first step to identify genes involved in bones' response to unloading, we evaluated the effects of unloading in eight inbred mouse strains: C57BL/6J, PWK/PhJ, WSB/EiJ, A/J, 129S1/SvImJ, NOD/ShiLtJ, NZO/HlLtJ, and CAST/EiJ. C57BL/6J and NOD/ShiLtJ mice had the greatest unloading-induced loss of diaphyseal cortical bone volume and strength. NZO/HlLtJ mice had the greatest metaphyseal trabecular bone loss, and C57BL/6J, WSB/EiJ, NOD/ShiLtJ, and CAST/EiJ mice had the greatest epiphyseal trabecular bone loss. Bone loss in the epiphyses displayed the highest heritability. With immobilization, mineral:matrix was reduced, and carbonate:phosphate and crystallinity were increased. A/J mice displayed the greatest unloading-induced loss of mineral:matrix. Changes in gene expression in response to unloading were greatest in NOD/ShiLtJ and CAST/EiJ mice. The most upregulated genes in response to unloading were associated with increased collagen synthesis and extracellular matrix formation. Our results demonstrate a strong differential response to unloading as a function of strain. Diversity outbred (DO) mice are a high-resolution mapping population derived from these eight inbred founder strains. These results suggest DO mice will be highly suited for examining the genetic basis of the skeletal response to unloading.

1. Introduction

Unloading of limbs due to prolonged bedrest, immobilization, or exposure to microgravity, decreases bone volume and strength, making bone more susceptible to fracture (Lang et al., 2017; Judex et al., 2004). However, the underlying mechanisms that lead to bone loss from unloading remain largely unknown. In both humans and mice, bone mineral density is highly heritable (Weaver et al., 2016; Price et al., 2005; Wergedal et al., 2005; Morris et al., 2019). Additionally, in mice the response to changes in mechanical loading varies as a function of genetic background (Judex et al., 2004; Price et al., 2005; Amblard et al., 2003; Sankaran et al., 2017; Li et al., 2005; Zhong et al., 2005; Judex et al., 2013). Indeed, Judex et al. identified six quantitative trait loci (QTLs) for unloading-induced loss of BV/TV in the F2 offspring of a double cross between BALB/cByJ22 and C3H/HeJ23 mice (Judex et al., 2004). These QTL accounted for 21% of the variability in loss of BV/TV in response to unloading in the F2 mice. In a subsequent study, Judex et al. identified five QTLs for unloading-induced loss in cortical bone area in the F2 of the same cross (Judex et al., 2016). These QTLs accounted for 10% of the variability in cortical bone loss in response to unloading. These data strongly suggest genetic variability affects the response of bone to unloading. However, identifying which specific genes contribute to the variability in response to unloading is challenging as each QTL contains several hundred candidate genes, and low-resolution mapping approaches have made it difficult to pinpoint causal genes.

* Corresponding author at: Engineering Research Building, Room 4322B, 70 South Madison Street, Richmond, VA 23220, USA.
E-mail addresses: mafriedman@vcu.edu (M.A. Friedman), aa9gj@virginia.edu (A. Abood), bhavya.senwar@colorado.edu (B. Senwar), yzhang29@vcu.edu (Y. Zhang), crmaroni@vcu.edu (C.R. Maroni), virginia.ferguson@colorado.edu (V.L. Ferguson), crf2s@virginia.edu (C.R. Farber), hjdonahue@vcu.edu (H.J. Donahue).

https://doi.org/10.1016/j.bonr.2021.101140
Received 4 August 2021; Received in revised form 28 September 2021; Accepted 4 October 2021
Available online 9 October 2021

Diversity outbred (DO) mice are a recently developed high-resolution mapping population that enables gene discovery for traits such as the response of bone to unloading (Svenson et al., 2012). DO mice are derived from random cross-breeding eight founder strains including classical laboratory (C57BL/6J, A/J, 129S1/SvImJ, NOD/ShiLtJ, and NZO/HlLtJ) and wild-derived strains (PWK/PhJ, WSB/EiJ, and CAST/EiJ). These mouse strains were chosen to maximize genetic diversity (Chesler et al., 2008; Churchill et al., 2004). DO mice can be used to investigate the genetics of a wide range of complex diseases and may be used to investigate the response of bone to unloading.

Hindlimb suspension (HLS) is the most widely used model for inducing bone loss from unloading (Lloyd et al., 2014; Lloyd et al., 2012; Morey-Holton and Globus, 2002; Grimm et al., 2016) and results in decreases in cortical and trabecular bone volume as well as loss of bone structural and tissue strength in as little as three weeks. While HLS enables examination of bone's response to unloading, HLS is not ideal for studying DO mice since each mouse is not genetically identical. Any single DO mouse is a result of a random funnel breeding scheme with the eight DO founder strains; therefore no two DO mice have similar parental lineage. The single limb immobilization model can overcome this problem by only unloading one limb and using the contralateral limb from the same animal as a genetically identical control. This model has been used extensively to show decreases in muscle mass and protein synthesis and similar increases in muscle atrophy gene expression, relative to that of HLS after one week (Lloyd et al., 2014; Lang et al., 2012; Speacht et al., 2018). We have recently began using single limb immobilization for bone loss and found this model results in decreased femoral bone volume fraction (−32%) and ultimate stress (−21%) after three weeks (Friedman et al., 2019).

In anticipation of future QTL mapping studies using DO mice, we employed the single limb immobilization model, rather than HLS, to induce bone loss. Our goal was to quantify the heritiablity and evaluate the extent of variation in the response to unloading in the DO founders. We hypothesized that genetic variation would impact the response of bone to unloading after three weeks of single limb immobilization in the eight inbred DO mouse founder strains. To test this hypothesis, we evaluated the effects of single limb immobilization on C57BL/6J, PWK/PhJ, WSB/EiJ, A/J, 129S1/SvImJ, NOD/ShiLtJ, NZO/HlLtJ, and CAST/EiJ mice. Our results are the first to quantify heritability of the response of bone to unloading in the DO mouse founder strains.

2. Materials and methods

2.1. Animals

All animal procedures were performed with the approval of the Virginia Commonwealth University Institutional Animal Care and Use Committee. Six male mice of each of the inbred DO founder strains were purchased from the Jackson Laboratory (PWK/PhJ – stock #003715, WSB/EiJ – stock #001145, A/J – stock #000646, 129S1/SvImJ – stock #002448, NOD/ShiLtJ – stock #001976, NZO/HlLtJ – stock #002105, and CAST/EiJ – stock #000928) at between four and fourteen weeks of age. Mouse age, sex, sample size, and immobilization duration were determined based on previous results using single limb immobilization (Friedman et al., 2019). C57BL/6J (stock #000664) bone morphology and mechanical properties from that study were also included in the analysis for this study, along with new Raman spectroscopy and RNA sequencing of samples from those mice. All mice were kept in single housing upon arrival and for the duration of the study. Mice were fed Teklad LM-485 chow (Envigo) and water ad libitum. At sixteen weeks old, all mice had casts placed on their left hind limbs. Mice were sacrificed after three weeks in the casts.

2.2. Casting protocol

The left hind limb of each mouse was immobilized in a cast as previously described (Friedman et al., 2019). Mice were placed under general anesthesia, and surgical tape was wrapped around the left hind limb. A microcentrifuge tube, with the bottom end removed, was then glued onto the tape. The contralateral right hind limbs were not altered and were used as controls (Lang et al., 2012). All mice were able to move around the cages by dragging the immobilized limb or rotating the limb at the hip (Fig. 1).

2.3. Physical activity and food consumption

Physical activity and food consumed was observed over 24-hour periods, before and after immobilization. These observations were performed one week prior to casting and two weeks after casting. Video was recorded for 24 h and analyzed using the OpenField Matlab function developed by Patel et al. (Patel et al., 2014) Total distance traveled over 24 h was measured for each mouse. Food consumption was measured by weighing food in the cages before and after the 24-hour observation period.

2.4. Bone morphology

Femurs were harvested at sacrifice and stored at −20 °C in calcium buffer. The bones were scanned by micro-CT (Skyscan 1173, Bruker microCT) as previously described (Friedman et al., 2019). Bones were scanned at 8.6 μm voxel size, 70kVp, 114 microA, 1.0 mm Al filter, and 1200 ms integration time. Bones were reoriented along anatomical landmarks. A 180-μm slice of the mid-diaphysis (4 mm distal to the lesser trochanter) was used to measure cortical area (Ct.Ar), area fraction (Ct.Ar/Tt.Ar) and thickness (Ct.Th). Metaphyseal trabecular bone morphology was evaluated using a 750-μm slice taken 200 μm proximal from the epiphyseal growth plate. Computer-traced ROIs were used to measure bone volume fraction (BV/TV), trabecular thickness (Tb.Th), trabecular number (Tb.N) and trabecular separation (Tb.Sp) (Bouxsein et al., 2010). Epiphyseal trabecular bone morphology was measured using a 520-μm slice of the epiphysis with freehand-traced ROIs immediately distal to the growth plate.

2.5. Mechanical properties

All femurs were tested by three-point bending to failure under displacement control at 1.0 mm/min. Bones were loaded with the anterior side in tension on support spans of 8 mm. Stiffness (instantaneous slope of the linear portion of the load-displacement curve at 3.5 N load), yield load (load at loss of 10% of stiffness), ultimate load, yield displacement, ultimate displacement, and work were measured (Jepsen

Fig. 1. A/J mouse with its left hindlimb immobilized.

et al., 2015). Geometry measurements at the location of the fracture site in the micro-CT scans were used to normalize structural-level properties to give estimates of elastic modulus, yield stress, ultimate stress, yield strain, ultimate strain, and toughness (Turner and Burr, 1993).

2.6. Raman spectroscopy

Raman spectroscopy was performed on the periosteum (Newman et al., 2014) of the distal aspect of the mid-diaphysis of the femurs, on the anterior side, 0.5 mm from the fractured surface from 3-point bending, with a Renishaw inVIA confocal Raman spectroscope (Renishaw, Wotton-under-Edge, Gluocestershire, UK; 785 nm wavelength laser, 6 s exposure time, 10 accumulations and 100% intensity). Bones were wrapped in gauze soaked in calcium buffer and stored at −20 °C. Prior to data collection, samples were thawed for 1 h and gently cleaned with a soft toothbrush to remove the periosteal surface and remaining soft tissue. The samples were not otherwise polished. Raman measurements were collected in a 2D map (3 × 20 sites with 20 μm spacing) that was aligned along the bone's long axis (Oest et al., 2016). All samples were evaluated while submerged in PBS. Peaks were centered around 1000 Raman shift/cm. The fluorescence baseline from all the spectra were subtracted, using an 11th order polynomial fit to the entire spectrum, followed by cosmic ray removal in the Renishaw Wire software. These spectra also underwent normalization. Custom MATLAB code was used to calculate peak area ratios of v2 phosphate:amide III or mineral:matrix ((413–466)/(1218–1309)cm^{-1}), carbonate:v1 phosphate or carbonate:phosphate ((1057–1104)/(917–984)cm^{-1}), and crystallinity (inverse of half-width at full maximum height of the v1 phosphate peak at 959 cm^{-1}) as in Fig. 2 (Akkus et al., 2004; Makowski et al., 2013; Awonusi et al., 2007). Data points from samples with low signal-to-noise ratios or data points which fell on residual soft tissue were removed and excluded from the analysis.

2.7. RNA sequencing

The tibial diaphysis, without marrow, from immobilized and contralateral mice from the 8 DO founders ($n = 3$ per mouse strain/group) was isolated and total RNA isolated using Trizol. RNA quality was assessed using an Agilent 4200 TapeStation System. RNA was of sufficient quality (RIN > 5) for all samples except those from the A/J strain. RNA-seq libraries were generated using Illumina TruSeq Stranded mRNA Library Prep kits and sequenced on an Illumina NextSeq500 for the seven mouse strains with high-quality RNA. Raw reads were aligned to the reference *Mus Musculus* genome (GRCM38) using Hisat2 (Kim et al., 2015). Transcript assembly and quantification was conducted using StringTie (Pertea et al., 2015). Differential Gene Expression analysis was completed using EdgeR (Robinson et al., 2010). Gene Ontology (GO) terms were assigned using PANTHER (Fisher test with FDR correction at 0.05) (Mi et al., 2019).

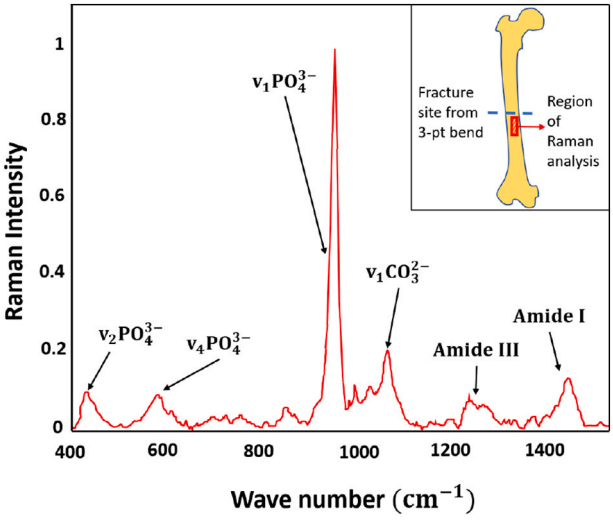

Fig. 2. Example Raman spectrum of a mouse femur and position of the Raman array on the periosteal surface of the femur.

2.8. Statistical analysis

Mixed effects analysis models (similar to repeated measures two-way ANOVAs) were used to test for significant ($p < 0.05$) main effects of mouse strain, immobilization, and interactions in GraphPad Prism. Sidak tests post-hoc were used to test for significant differences between control and immobilized limbs of each mouse strain. For Raman analysis, as multiple test sites were collected on each bone from Raman spectroscopy, a repeated measures mixed model analysis was performed in software JMP 14, with mouse strain (8 levels) and loading condition (2 levels) as fixed effects (with interaction term) and mouse number as a random effect. Tukey's post hoc was used to test for significant differences in various Raman parameters for the two fixed effects.

Narrow-sense heritability, the variance in the data due to genetic factors, was calculated for the magnitude of effects of immobilization on each property measured as previously described (Lariviere and Mogil, 2010; Falconer, 1996). Magnitude of effects of immobilization were determined by calculating percent differences between immobilized and contralateral control limbs. One-way ANOVAs with Tukey's tests post-hoc were used to test for significant differences in magnitude of effects of immobilization in GraphPad Prism. The R-squared values from the One-way ANOVAs were used as the heritability values since they represent the variation in the data from mouse strain.

3. Results

One WSB/EiJ mouse was removed from the study after it escaped from the cage for >12 h. Most mice spent the majority of their waking hours chewing on the casts. All casts that were removed by the mice were replaced within 24 h. Immobilized limbs had increased swelling and skin ulcers after three weeks.

3.1. Effects of immobilization on cortical and trabecular bone geometry were mouse strain-dependent

In cortical bone of the mid-diaphysis of the femur, mouse strain affected Ct.Ar, Tt.Ar, Ct.Ar/Tt.Ar, and Ct.Th, and immobilization affected Ct.Ar/Tt.Ar and Tt.Ar (Fig. 3). C57BL/6J was the mouse strain with the greatest difference between immobilized and control limbs for Ct.Ar/Tt.Ar, Ct.Ar, and Ct.Th (Supplemental Fig. S1). For CtAr/TtAr of individual strains, paired *t*-tests would need $n = 9$ for C57BL/6J, $n = 521$ for PWK/PhJ, $n = 347$ for WSB/EiJ, $n = 15$ for A/J, $n = 24$ for 129S1/SvImJ, $n = 14$ for NOD/ShiLtJ, $n = 64$ for NZO/HiLtJ, and $n = 2249$ for CAST/EiJ for alpha = 0.05, power = 0.8. Raw data is included in the supplemental file 'All Data'.

Mouse strain affected femoral metaphyseal BV/TV and Tb.N (Fig. 4). Immobilization and mouse strain had interactive effects on Tb. Th and Tb.Sp. In the femoral epiphysis, immobilization and mouse strain had interactive effects on BV/TV, Tb. Th, Tb. N, and Tb. Sp (Fig. 5). CAST/EiJ mice had the greatest difference in Tb.N between immobilized and contralateral control limbs, while C57BL/6J mice had the greatest difference in Tb.Th. WSB/EiJ mice had the greatest difference in Tb.Sp (Supplemental Fig. S3).

3.2. Mouse strain and immobilization influenced bone strength but to a lesser extent than bone geometry

Mouse strain affected all femoral structural-level and tissue-level mechanical properties (Fig. 6). Immobilization affected ultimate stress

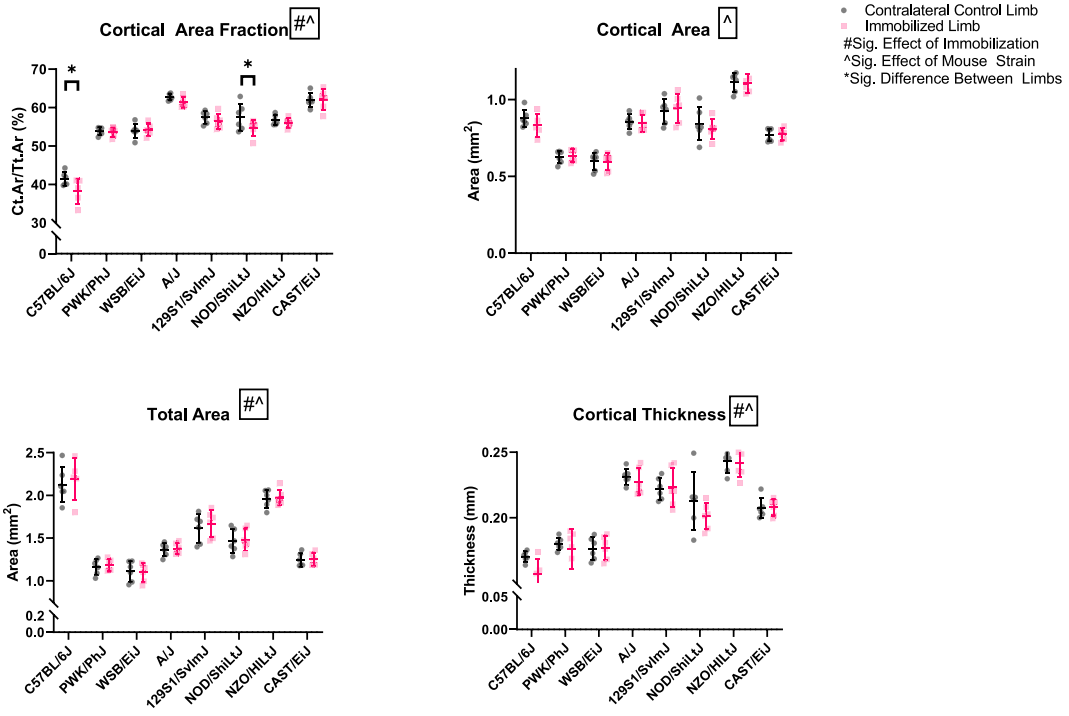

Fig. 3. Femoral (mean ± SD) cortical bone of the mid-diaphysis after three weeks of single limb immobilization (n = 5–6 per mouse strain). There was a significant main effect of mouse strain on every property ($p < 0.0001$), and there was a significant main effect of immobilization ($p < 0.05$) on Ct.Ar/Tt.Ar, total area, and cortical thickness. C57BL/6J and NOD/ShiLtJ mice had decreased Ct.Ar/Tt.Ar from immobilization ($p < 0.05$). The other mouse strains had no significant differences between immobilized and contralateral control limbs.

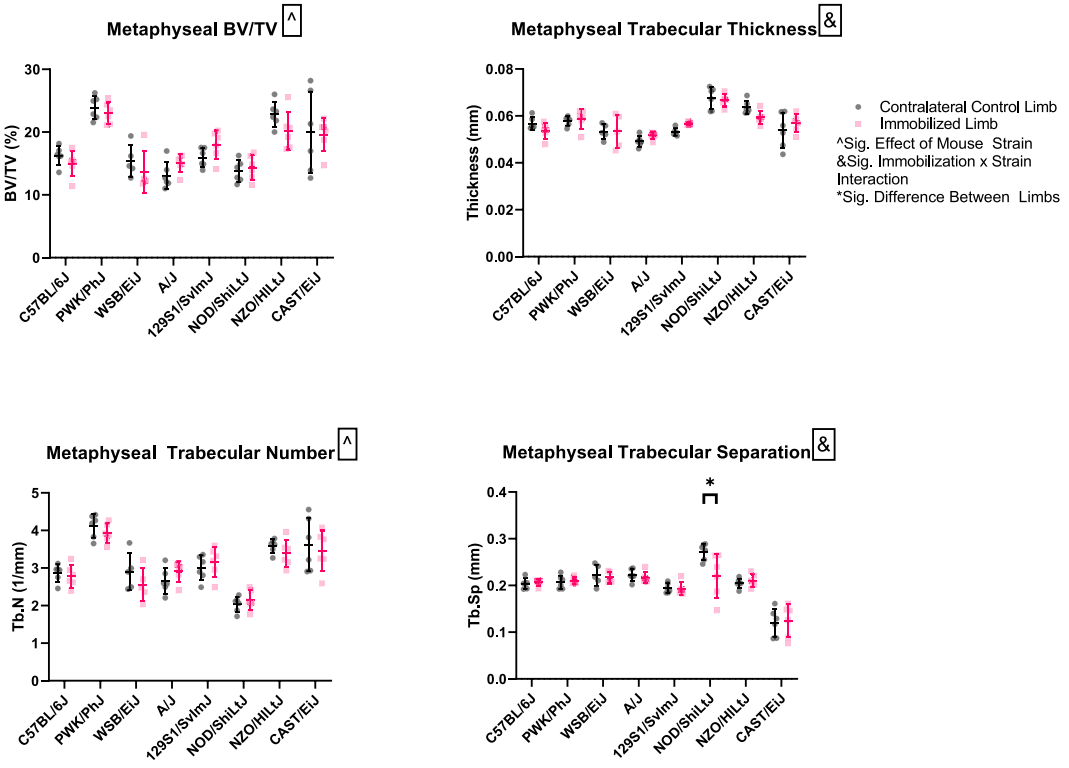

Fig. 4. Femoral (mean ± SD) trabecular bone of the distal metaphysis after three weeks of single limb immobilization ($n = 5–6$ per mouse strain). There were significant main effects of mouse strain ($p < 0.05$) on BV/TV and Tb.N. There was a significant immobilization and mouse strain interaction ($p < 0.05$) for Tb.Th and Tb.Sp. NOD/ShiLtJ mice had greater Tb.Sp in immobilized limbs than contralateral control limbs ($p < 0.05$).

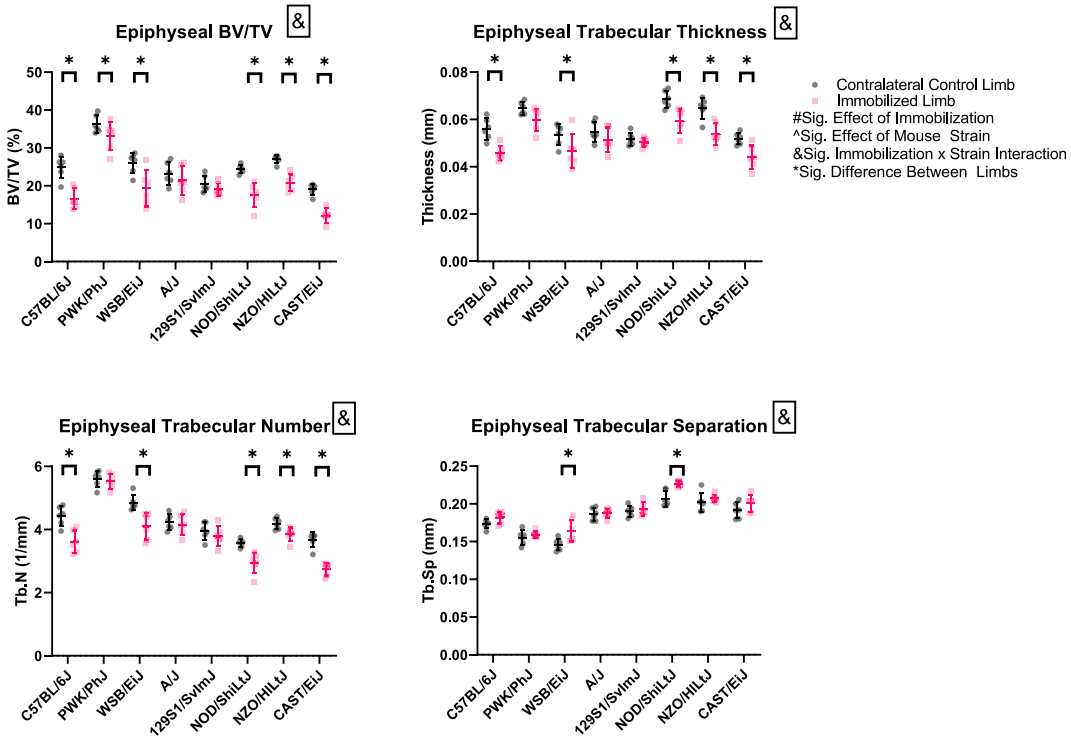

Fig. 5. Femoral (mean ± SD) trabecular bone of the distal epiphysis after three weeks of single limb immobilization (n = 5–6 per mouse strain). There was a significant immobilization and mouse strain interaction ($p < 0.05$) for all properties. All mouse strains had lower epiphyseal BV/TV in immobilized limbs vs. contralateral control limbs ($0.05 < p < 0.0001$) except A/J and 129S1/SvImJ.

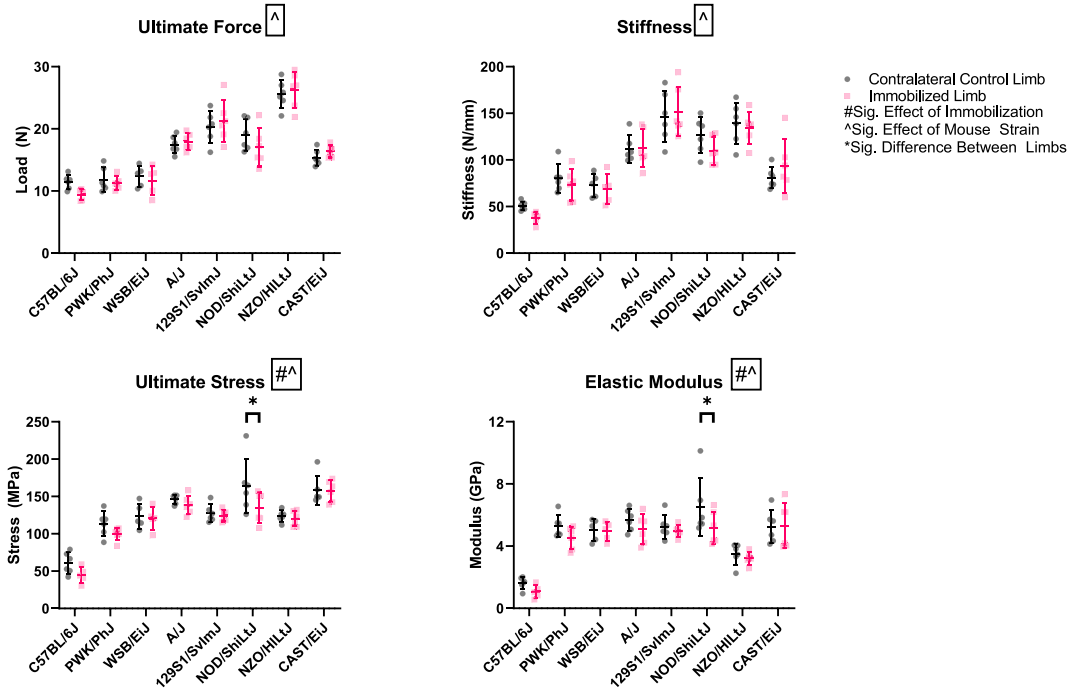

Fig. 6. Femoral (mean ± SD) bone structural-level and tissue-level strength after three weeks of single limb immobilization, measured by three-point bending to failure ($n = 5–6$ per mouse strain). There was a significant main effect of immobilization ($p < 0.05$) on ultimate stress and elastic modulus. There was a significant main effect of mouse strain ($p < 0.05$) on all properties. Only NOD/ShiLtJ mice had loss of ultimate stress and elastic modulus ($p < 0.05$) from immobilization.

and elastic modulus. NOD/ShiLtJ mice had lower ultimate stress in immobilized limbs versus control limbs ($p < 0.05$). Raw data is included in the supplemental file 'All Data'.

3.3. Mouse strain and immobilization both influenced bone material quality

Mouse strain and immobilization both affected Raman spectroscopy

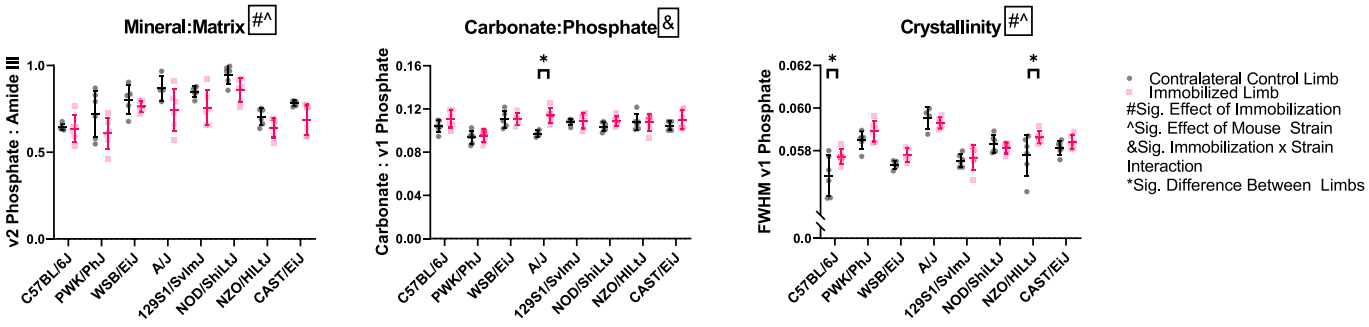

Fig. 7. Femoral (mean ± SD) cortical bone mineral:matrix, carbonate:phosphate and crystallinity measured by Raman spectroscopy after three weeks of single limb immobilization (n = 5–6 per mouse strain). There were significant main effects of immobilization and mouse strain ($p < 0.05$) on mineral:matrix and crystallinity. There was a significant ($p < 0.05$) immobilization and mouse strain interaction on carbonate:phosphate. A/J mice had increased carbonate:phosphate, and NZO/HiLtJ mice had increased crystallinity from immobilization ($p < 0.05$).

measures of mineral:matrix and crystallinity (Fig. 7). There was an interactive effect of mouse strain and immobilization on carbonate:phosphate ratios. Immobilized limbs of 129S1/SvImJ, A/J, CAST/EiJ, NOD/ShiLtJ, PWK/PhJ, WSB/EiJ and NZO/HiLtJ mice had lower mineral:matrix ratio than control limbs, though not statistically significant. Immobilized limbs of A/Jmice had significantly greater carbonate:phosphate ratio than control limbs. Crystillanity was the greatest in the control limbs of the A/J mice among the mouse strains, while C57BL/6J mice had the lowest. Crystallinity significantly increased with immobilization in NZO/HiLtJ and C57BL/6J mice. Raw data is included in the supplemental file 'All Data'.

3.4. RNA-seq revealed gene expression was affected by immobilization in some but not all mouse strains after three weeks

There were 414 genes differentially expressed in response to immobilization across seven of the eight DO founders (FDR < 0.05, Fig. 8). CAST/EiJ mice had the greatest number of genes, 1095, differentially expressed between immobilized and control limbs. NOD/ShiLtJ mice had 788, and PWK/PhJ had 19 genes differentially expressed between immobilized and control limbs. No other mouse strains had genes differentially expressed between immobilized and control limbs. Among the genes affected by immobilization, the genes with the highest expression in immobilized limbs were *Col1a2*, *Col1a1*, *Sparc*, *Spp1*, and *Col5a2*. Gene ontology analysis revealed the most highly upregulated

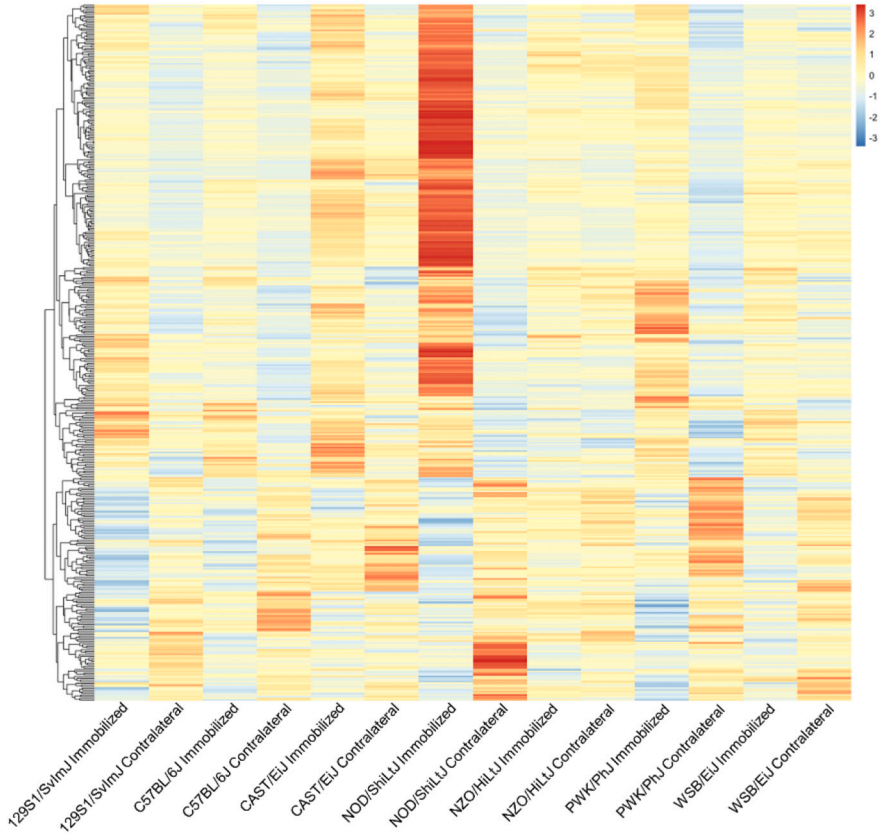

Fig. 8. Heatmap showing relative gene expression of 414 genes affected by immobilization (FDR < 0.05), as measured by RNA-seq ot tibial diaphyseal samples from immobilized and contralateral control limbs (n = 3 per mouse strain). Each row represents one gene. NOD/ShiLtJ and CAST/EiJ mice had the greatest number of genes affected by immobilization (FDR < 0.05).

Table 1
Gene ontology analysis of the most highly upregulated pathways in immobilized limbs compared to contralateral control limbs.

Reactome pathways	(raw *P*-value)	(FDR)
Collagen formation (R-MMU-1474290)	2.01E-21	3.25E-18
Collagen biosynthesis and modifying enzymes (R-MMU-1650814)	2.54E-19	2.05E-16
Extracellular matrix organization (R-MMU-1474244)	2.02E-18	1.09E-15
Assembly of collagen fibrils and other multimeric structures (R-MMU-2022090)	1.08E-12	4.37E-10
Degradation of the extracellular matrix (R-MMU-1474228)	6.55E-11	2.12E-08

pathways in immobilized limbs to be pathways involved in collagen formation, collagen assembly, and extracellular matrix organization (Table 1). There were 8568 genes differentially expressed across the seven DO founders. Full list of differentially expressed genes and gene ontology analysis are in the supplemental file 'All Data'.

3.5. All mouse strains lost body weight from immobilization

All mouse strains lost body weight as a result of the immobilization (Table 2). Weight loss ranged from −2.6% body weight in PWK/PhJ mice to −17% in A/J mice. Mouse cage activity, measured in total distance traveled, decreased greatly in A/J mice after immobilization. All other mouse strains had slight decreases or large increases in distance traveled. Food consumption increased in all mouse strains except NZO/H1LtJ.

3.6. Heritability of effects of immobilization varied by region of the bone

Heritability, the variance in the data due to genetic factors, was calculated for each property measured as previously described (Table 3) (Lariviere and Mogil, 2010; Falconer, 1996). Each heritability value shows the effects of genetic variation on the response to immobilization for that property. Loss of epiphyseal Tb.N had the highest heritability at 71%, followed by loss of epiphyseal BV/TV at 64%. This suggests changes in these properties in response to immobilization are influenced by genetic variation. Mineral:matrix had the lowest heritability at 16%. These data suggest the response of bone to unloading is influenced by genetic differences among the DO founder strains.

4. Discussion

The DO mouse population is emerging as a potential tool for evaluating the role of genetic variation on bone adaptation. This is the first study to examine the effects of mechanical unloading on the eight inbred DO founder strains. Our results showing variation in the response to unloading among the founder strains suggest that single limb immobilization can be used on DO mice to study the role of genetic variation on bone's response to unloading.

Table 3
Heritability of the response of each property to immobilization.

Property	Heritability
Weight Loss	62%
Cage activity	24%
Food consumption	21%
Ct.Ar/Tt.Ar	31%
Ct.Ar	15%
Ct.Th	21%
Metaphyseal BV/TV	27%
Metaphyseal Tb.Th	35%
Metaphyseal Tb.N	23%
Epiphyseal BV/TV	64%
Epiphyseal Tb.Th	35%
Epiphyseal Tb.N	71%
Ultimate Force	26%
Ultimate Stress	28%
Mineral:Matrix	16%
Carbonate:Phosphate	30%
Crystallinity	28%

In this study, we observed that genetic background played a major role in the response of bone to immobilization. C57BL/6J, NOD/ShiLtJ, and CAST/EiJ mice demonstrated differences in bone geometry and/or gene expression in response to immobilization, while the other five mouse strains had few or no differences. This variety of effects suggests there may be genes that protect bone from the negative effects of unloading. Heritability values for the responses of each bone property to immobilization ranged from 15 to 71%. These values indicate that genetic variation among DO founder strains represented a significant source of variation in the response. This highlights the large systemic effects of genetic variation on the ability of bone to sense and respond to mechanical unloading. Importantly, these data suggest that future studies utilizing a population of DO mice should lead to the identification of QTL, and ultimately individual genes, that influence the unloading response in bone.

C57BL/6J and NOD/ShiLtJ mice had the greatest percent differences in diaphyseal cortical bone from unloading. As would be expected from these differences, these mice also had the greatest percent differences in bone ultimate force from unloading. NZO/HlLtJ mice had the greatest percent differences from unloading in metaphyseal trabecular bone, and C57BL/6J, WSB/EiJ, NOD/ShiLtJ, and CAST/EiJ mice had the greatest percent differences from unloading in epiphyseal trabecular bone. Regional differences in unloading effects may be due to differences in bone morphology, animal size, changes in gait, and activity levels, all of which are affected by genetic differences. That region-specific response to unloading may be influenced by genetics is an intriguing concept that requires further investigation.

Table 2
Mouse body weight, food consumption, and cage activity measurements (n = 5–6 per mouse strain).

Mouse Strain	C57Bl/6J	PWK/PhJ	WSB/EiJ	A/J	129S1/SvImJ	NOD/ShiLtJ	NZO/HlLtJ	CAST/EiJ
Day 1 Weight (g)	29.7 ± 2.5	19.0 ± 0.8	16.3 ± 1.5	27.5 ± 2.0	28.4 ± 1.8	30.5 ± 2.9	48.9 ± 4.0	17.0 ± 0.9
Day 21 Weight (g)	26.9 ± 2.2	18.5 ± 1.0	15.7 ± 1.3	22.9 ± 1.8	25.3 ± 1.5	27.7 ± 1.1	42.3 ± 3.4	15.8 ± 0.8
% Change	−9.2%	−2.6%	−3.9%	−17%	−11%	−8.7%	−13%	−7.3%
p-value (paired *t*-test)	0.022	0.087	0.032	0.0002	0.001	0.015	0.0002	0.012
Baseline activity (km/day)	2.35 ± 0.91	5.49 ± 1.84	N/A	2.34 ± 0.52	1.91 ± 0.67	1.65 ± 0.88	1.49 ± 0.59	3.01 ± 1.09
Immobilized activity (km/day)	5.22 ± 2.16	7.70 ± 4.51	4.03 ± 3.18	0.90 ± 0.74	2.10 ± 0.72	2.11 ± 0.66	1.70 ± 0.79	2.69 ± 0.70
% Change	169%	47%	N/A	−57%	39%	94%	63%	−6%
p-value (paired t-test)	0.210	0.480	N/A	0.024	0.530	0.486	0.416	0.827
Baseline food consumption (g/day)	4.4 ± 0.9	2.2 ± 0.5	N/A	3.3 ± 0.7	4.5 ± 1.1	4.0 ± 0.4	5.0 ± 0.5	3.7 ± 2.0
Immobilized food consumption (g/day)	5.2 ± 0.6	3.3 ± 1.0	2.0 ± 1.3	4.4 ± 1.3	5.7 ± 1.6	4.9 ± 0.6	5.0 ± 1.5	4.4 ± 2.2
% Change	26%	65%	N/A	43%	33%	24%	−1.6%	22%
p-value (paired t-test)	0.031	0.129	N/A	0.175	0.176	0.004	0.886	0.149

The greatest overall effects of immobilization were seen in the femoral epiphysis, not in the metaphysis. A previous study of bone loss from hindlimb suspension in C57BL/6J mice showed few effects on femoral methaphyseal bone, but epiphyseal bone loss was not quantified in that study (Lloyd et al., 2014). Epiphyseal bone may be uniquely positioned to suffer bone loss from immobilization as this region has a greater amount of trabecular bone, and epiphyseal bone could experience a large decrease in mechanical loading following the removal (or reduction) of joint contact forces. Unloading also reduces chondrocyte growth and differentiation which may negatively affect bone metabolism in the epiphysis (Sibonga et al., 2000; Klement and Spooner, 1999). A previous study of bone loss from hindlimb suspension using three different strains of mice showed lesser effects of unloading in C57BL/6J mice than were seen here (Judex et al., 2004), suggesting immobilization from casting may be more effective at causing epiphyseal bone loss than hindlimb suspension which does not immobilize the knee joint. Bone loss in the epiphysis had the highest heritability in this study, suggesting a greater influence of genetics in this region. There is sparse data on epiphyseal bone changes in response to immobilization in mice in the literature (Mirtz et al., 2011). This narrow region of bone requires very high resolution CT scanning to produce ROIs large enough for accurate measurement of 3D trabecular bone properties (Bouxsein et al., 2010). As several factors may affect bone metabolism in the epiphysis, the epiphysis may be a region of high interest for future research on effects of unloading on bone.

While bone material quality has been linked to genetic background in mice (Courtland et al., 2008), this is the first study to examine bone material quality measurements in a large number of genetically diverse, inbred mouse strains exposed to mechanical unloading. Mineral chemistry measures varied greatly across the eight mouse strains, and bone quality responded to immobilization in a mouse strain-specific manner. With immobilization, bone chemistry measures followed a general pattern of lower mineral:matrix, increased carbonation (carbonate:phosphate), and increased crystallinity. Unloading at osteoporotic fracture sites in postmenopausal women resulted in diminished mineral:matrix (McCreadie et al., 2006). Similarly, growing rats exposed to 12.5 days of microgravity on COSMOS 1179, a spaceflight experiment, had reduced apatite mineral and bone stiffness (Simmons et al., 1990). Such compositional changes in bone, along with increased carbonate:phosphate and crystallinity with immobilization, may contribute to decreased bone strength. Carbonation, which increases with tissue age, has been shown to increase in femoral trabecular bone of women who had an osteoporotic fracture and in adult female rats following hindlimb unloading (McCreadie et al., 2006; Peres-Ueno et al., 2017). Increased substitution of carbonate in the hydroxyapatite crystals in the bone can cause asymmetry in the crystal lattice, making the bone more prone to damage under mechanical stress (Baig et al., 1999; Handschin and Stern, 1992). Smaller mineral crystals enable greater deformation of mineralized collagen fibers, thus leading to higher post-yield deformation and reducing propensity toward fracture. In contrast, increased crystallinity contributes to poor bone strength where larger crystals increase the brittleness of bone (Yerramshetty and Akkus, 2008). Crystallinity and brittleness has also been shown to increase with age (Freeman et al., 2001) and, in some studies, with unloading from microgravity exposure (Simmons et al., 1990; Peres-Ueno et al., 2017; Patterson-Buckendahl et al., 1987a). Thus, these changes in bone chemistry may contribute to impaired fracture toughening mechanisms and reduce bone strength. As the changes to bone chemistry and bone geometry measures due to immobilization are mouse strain-specific (Courtland et al., 2008), this indicates that the DO population holds potential to reveal specific genes that may play roles in preventing detrimental bone chemistry alterations that occur with disuse.

Changes in gene expression in response to unloading were greatest in NOD/ShiLtJ and CAST/EiJ mice. These results are different from diaphyseal cortical bone geometry data that showed the greatest effects of unloading in C57BL/6J mice. This may reflect a timing issue where C57BL/6J mice have more differentially expressed genes in response to unloading at an earlier time point and have reached some homeostasis after three weeks. Measuring gene expression data does have the limitation of only analyzing expression at one moment in time when gene expression fluctuates greatly throughout the day and from week to week. Additionally, we measured gene expression in the tibia and bone geometry in the femur, so there may have been bone-specific differences in the response to unloading. Alternatively, differences in measurement variance within each mouse strain may have made statistically significant differences difficult to detect for this study's sample size. All of these differences highlight the influence of genetic variation on the timing and location of the skeletal response to unloading.

Interestingly, the gene ontology pathways shown to be most highly upregulated in response to unloading were pathways associated with increasing collagen synthesis and extracellular matrix formation. This is similar to the response seen after anabolic mechanical loading (Morse et al., 2018; Govey et al., 2015; Galea et al., 2017). This was one of the first studies to use RNAseq to examine changes in gene expression in bone in response to unloading and to compare gene expression across multiple mouse strains (Ayturk, 2019). There were some limitations as we were only able to analyze seven of the mouse strains, and gene expression was analyzed in the tibia while all other measurements were done in the femur. Further studies need to be performed to better understand the time course of changes in gene activation with changes in mechanical loading and how genetic variation affects these responses.

We did not detect changes in physical activity in the mouse strains that had the greatest bone loss. Physical activity increased in most mouse strains after immobilization. Although the casts made ambulation more difficult and cumbersome, the mice appeared to be more active by trying to free themselves from the casts. A/J mice had decreased activity, but that did not translate to bone loss as A/J mice were one of the least affected mouse strains. This can be a limitation of the activity level measurement which only showed distance traveled and did not take into account changes in gait or speed which could affect bone loss (Taylor and C, 1986). Surprisingly, food consumption increased for most of the mouse strains, a result that would not be expected to be associated with bone loss (Artiga et al., 2007). Other changes in mouse behavior not measured may be able to partially explain the bone loss from immobilization in this study.

Since differences in the response to immobilization were found among the eight inbred DO founder strains, we would expect to see differences in the response to immobilization in DO mice. A sham group of mice was not used. Our previous work in younger C57BL/6J mice indicated single limb immobilization causes bone loss in the immobilized limbs and the control limbs (Friedman et al., 2019). However, our purpose here was to show how the eight DO founder strains respond differently to immobilization, not to further examine the immobilization model. Baseline CT scans were not taken, so we cannot confirm that immobilized limbs lost bone, as opposed to naturally having significantly lower bone volume. This also limits our ability to determine if all mice in all mouse strains had reached skeletal maturity or if some strains were still in development. Seven of the mouse strains we used have not been studied as extensively as the C57BL/6J mice to determine what age they reach skeletal maturity. We chose the age of 16 weeks based on when C57BL/6J mice reach peak bone volume (Glatt et al., 2007). We did not include female mice in this study. Previous rodent unloading studies indicated greater bone loss in males than females (David et al., 2006; Hefferan et al., 2003), so we used males here to reduce the number of animals needed. Future studies using DO mice should include both male and female mice to uncover sex differences in the effects of genetic variation.

Genetic variation plays a major role in the accrual and maintenance of bone mass. Here we showed genetic variation in mice influenced differences in the skeletal response to unloading from immobilization. There were mouse strain-dependent differences in gene expression and in changes to bone volume, bone strength, and bone material quality

from immobilization. Identification of which genes are responsible for unloading-induced bone changes would be better done in the DO mice which provide greater power to detect significant genes. We should next evaluate the response to immobilization in DO mice and use that information to uncover novel genes involved for protecting bone from the negative effects of unloading.

CRediT authorship contribution statement

Michael A. Friedman: Conceptualization, Data curation, Formal analysis, Investigation, Methodology, Validation, Visualization, Supervision, Writing – original draft, Writing – review & editing. **Abdullah Abood:** Data curation, Formal analysis, Investigation, Methodology, Visualization, Writing – review & editing. **Bhavya Senwar:** Data curation, Formal analysis, Investigation, Methodology, Visualization, Writing – review & editing. **Yue Zhang:** Investigation. **Camilla Reina Maroni:** Investigation. **Virginia L. Ferguson:** Conceptualization, Formal analysis, Funding acquisition, Project administration, Resources, Supervision, Writing – review & editing. **Charles R. Farber:** Conceptualization, Formal analysis, Funding acquisition, Project administration, Resources, Supervision, Writing – review & editing. **Henry J. Donahue:** Conceptualization, Formal analysis, Validation, Funding acquisition, Project administration, Resources, Supervision, Writing – review & editing.

Declaration of competing interest

None.

Acknowledgments

This work is supported by the National Institutes of Health (R01AR068132-20, 5R01AR068345, R01AR071657, T32LM012416), National Science Foundation (NSF CBET 1338154), National Aeronautics and Space Administration (80NSSC18K1473), and the Translational Research Institute for Space Health Postdoctoral Fellowship (NASA Cooperative Agreement NNX16AO69A).

Appendix A. Supplementary data

Supplementary data to this article can be found online at https://doi.org/10.1016/j.bonr.2021.101140.

References

Akkus, O., Adar, F., Schaffler, M.B., 2004. Age-related changes in physicochemical properties of mineral crystals are related to impaired mechanical function of cortical bone. Bone 34 (3), 443–453.

Amblard, D., Lafage-Proust, M.H., Laib, A., Thomas, T., Ruegsegger, P., Alexandre, C., Vico, L., 2003. Tail suspension induces bone loss in skeletally mature mice in the C57BL/6J strain but not in the C3H/HeJ strain. J. Bone Miner. Res. 18 (3), 561–569.

Artiga, A.I., Viana, J.B., Maldonado, C.R., Chandler-Laney, P.C., Oswald, K.D., Boggiano, M.M., 2007. Body composition and endocrine status of long-term stress-induced binge-eating rats. Physiol. Behav. 91 (4), 424–431.

Awonusi, A., Morris, M.D., Tecklenburg, M.M., 2007. Carbonate assignment and calibration in the Raman spectrum of apatite. Calcif. Tissue Int. 81 (1), 46–52.

Ayturk, U., 2019. RNA-seq in skeletal biology. Curr. Osteoporos. Rep. 17 (4), 178–185.

Baig, A.A., Fox, J.L., Young, R.A., Wang, Z., Hsu, J., Higuchi, W.I., Chhettry, A., Zhuang, H., Otsuka, M., 1999. Relationships among carbonated apatite solubility, crystallite size, and microstrain parameters. Calcif. Tissue Int. 64 (5), 437–449.

Bouxsein, M.L., Boyd, S.K., Christiansen, B.A., Guldberg, R.E., Jepsen, K.J., Muller, R., 2010. Guidelines for assessment of bone microstructure in rodents using micro-computed tomography. J. Bone Miner. Res. 25 (7), 1468–1486.

Chesler, E.J., Miller, D.R., Branstetter, L.R., Galloway, L.D., Jackson, B.L., Philip, V.M., Voy, B.H., Culiat, C.T., Threadgill, D.W., Williams, R.W., Churchill, G.A., Johnson, D. K., Manly, K.F., 2008. The collaborative cross at oak Ridge National Laboratory: developing a powerful resource for systems genetics. Mamm. Genome 19 (6), 382–389.

Churchill, G., Airey, D.C., Allayee, H., Angel, J.M., Attie, A.D., Beatty, J., Beavis, W.D., Belknap, J.K., Bennett, B., Berrettini, W., Bleich, A., Bogue, M., Broman, K.W., Buck, K.J., Buckler, E., Burmeister, M., Chesler, E.J., Cheverud, J.M., Clapcote, S., Cook, M.N., Cox, R.D., Crabbe, J.C., Crusio, W.E., Darvasi, A., Deschnepper, C.F., Doerge, R.W., Farber, C.R., Forejt, J., Gaile, D., Garlow, S.J., Geiger, H., Gershenfeld, H., Gordon, T., Gu, J., Gu, W.K., de Haan, G., Hayes, N.L., Heller, C., Himmelbauer, H., Hitzemann, R., Hunter, K., Hsu, H.C., Iraqi, F.A., Ivandic, B., Jacob, H.J., Jansen, R.C., Jjepsen, K.J., Johnson, D.K., Johnson, T.E., Kempermann, G., Kendziorski, C., Kotb, M., Kooy, R.F., Llamas, B., Lammert, F., Lassalle, J.M., Lowenstein, P.R., Lu, L., Lusiss, A., Manly, K.F., Marcucio, R., Matthews, D., Medrano, J.F., Miller, D.R., Mittleman, G., Mock, B.A., Mogil, J.S., Montagutelli, X., Morahan, G., Morris, D.G., Mott, R., Nadeau, J.H., Nagase, H., Nowakowski, R.S., O'Hara, B.F., Osadchuk, A.V., Page, G.P., Paigen, B., Paigen, K., Palmer, A.A., Pan, H.J., Peltonen-Palotie, L., Peirce, J., Pomp, D., Pravenec, M., Prows, D.R., Qi, Z.H., Reeves, R.H., Roder, J., Rosen, G.D., Schadt, E.E., Schalkwyk, L.C., Seltzer, Z., Shimomura, K., Shou, S.M., Sillanpaa, M.J., Siracusa, L. D., Snoeck, H.W., Spearow, J.L., Svenson, K., Tarantino, L.M., Threadgill, D., Toth, L. A., Valdar, W., de Villena, F.P.M., Warden, C., Whatley, S., Williams, R.W., Wiltshire, T., Yi, N.J., Zhang, D.B., Zhang, M., Zou, F., C. Complex Trait, 2004. The Collaborative Cross, a community resource for the genetic analysis of complex traits. Nature Genet. 36 (11), 1133–1137.

Courtland, H.W., Nasser, P., Goldstone, A.B., Spevak, L., Boskey, A.L., Jepsen, K.J., 2008. Fourier transform infrared imaging microspectroscopy and tissue-level mechanical testing reveal intraspecies variation in mouse bone mineral and matrix composition. Calcif. Tissue Int. 83 (5), 342–353.

David, V., Lafage-Proust, M.H., Laroche, N., Christian, A., Ruegsegger, P., Vico, L., 2006. Two-week longitudinal survey of bone architecture alteration in the hindlimb-unloaded rat model of bone loss: sex differences. Am. J. Physiol. Endocrinol. Metab. 290 (3), E440–E447.

Falconer, D.S., 1996. Prentice Hall, Harlow, England.

Freeman, J.J., Wopenka, B., Silva, M.J., Pasteris, J.D., 2001. Raman spectroscopic detection of changes in bioapatite in mouse femora as a function of age and in vitro fluoride treatment. Calcif. Tissue Int. 68 (3), 156–162.

Friedman, M.A., Zhang, Y., Wayne, J.S., Farber, C.R., Donahue, H.J., 2019. Single limb immobilization model for bone loss from unloading. J. Biomech. 83, 181–189.

Galea, G.L., Meakin, L.B., Harris, M.A., Delisser, P.J., Lanyon, L.E., Harris, S.E., Price, J. S., 2017. Old age and the associated impairment of bones' adaptation to loading are associated with transcriptomic changes in cellular metabolism, cell-matrix interactions and the cell cycle. Gene 599, 36–52.

Glatt, V., Canalis, E., Stadmeyer, L., Bouxsein, M.L., 2007. Age-related changes in trabecular architecture differ in female and male C57BL/6J mice. J. Bone Miner. Res. 22 (8), 1197–1207.

Govey, P.M., Kawasawa, Y.I., Donahue, H.J., 2015. Mapping the osteocytic cell response to fluid flow using RNA-seq. J. Biomech. 48 (16), 4327–4332.

Grimm, D., Grosse, J., Wehland, M., Mann, V., Reseland, J.E., Sundaresan, A., Corydon, T.J., 2016. The impact of microgravity on bone in humans. Bone 87, 44–56.

Handschin, R.G., Stern, W.B., 1992. Crystallographic lattice refinement of human bone. Calcif. Tissue Int. 51 (2), 111–120.

Hefferan, T.E., Evans, G.L., Lotinun, S., Zhang, M., Morey-Holton, E., Turner, R.T., 2003. Effect of gender on bone turnover in adult rats during simulated weightlessness. J. Appl. Physiol. (1985) 95 (5), 1775–1780.

Jepsen, K.J., Silva, M.J., Vashishth, D., Guo, X.E., van der Meulen, M.C., 2015. Establishing biomechanical mechanisms in mouse models: practical guidelines for systematically evaluating phenotypic changes in the diaphyses of long bones. J. Bone Miner. Res. 30 (6), 951–966.

Judex, S., Garman, R., Squire, M., Busa, B., Donahue, L.R., Rubin, C., 2004. Genetically linked site-specificity of disuse osteoporosis. J. Bone Miner. Res. 19 (4), 607–613.

Judex, S., Zhang, W., Donahue, L.R., Ozcivici, E., 2013. Genetic loci that control the loss and regain of trabecular bone during unloading and reambulation. J. Bone Miner. Res. 28 (7), 1537–1549.

Judex, S., Zhang, W., Donahue, L.R., Ozcivici, E., 2016. Genetic and tissue level muscle-bone interactions during unloading and reambulation. J. Musculoskelet. Neuronal Interact. 16 (3), 174–182.

Kim, D., Langmead, B., Salzberg, S.L., 2015. HISAT: a fast spliced aligner with low memory requirements. Nat. Methods 12 (4), 357–360.

Klement, B.J., Spooner, B.S., 1999. Mineralization and growth of cultured embryonic skeletal tissue in microgravity. Bone 24 (4), 349–359.

Lang, S.M., Kazi, A.A., Hong-Brown, L., Lang, C.H., 2012. Delayed recovery of skeletal muscle mass following hindlimb immobilization in mTOR heterozygous mice. PLoS One 7 (6), e38910.

Lang, T., Van Loon, J., Bloomfield, S., Vico, L., Chopard, A., Rittweger, J., Kyparos, A., Blottner, D., Vuori, I., Gerzer, R., Cavanagh, P.R., 2017. Towards human exploration of space: the THESEUS review series on muscle and bone research priorities. NPJ Microgravity 3, 8.

Lariviere, W.R., Mogil, J.S., 2010. The genetics of pain and analgesia in laboratory animals. Methods Mol. Biol. 617, 261–278.

Li, C.Y., Schaffler, M.B., Wolde-Semait, H.T., Hernandez, C.J., Jepsen, K.J., 2005. Genetic background influences cortical bone response to ovariectomy. J. Bone Miner. Res. 20 (12), 2150–2158.

Lloyd, S.A., Lewis, G.S., Zhang, Y., Paul, E.M., Donahue, H.J., 2012. Connexin 43 deficiency attenuates loss of trabecular bone and prevents suppression of cortical bone formation during unloading. J. Bone Miner. Res. 27 (11), 2359–2372.

Lloyd, S.A., Lang, C.H., Zhang, Y., Paul, E.M., Laufenberg, L.J., Lewis, G.S., Donahue, H. J., 2014. Interdependence of muscle atrophy and bone loss induced by mechanical unloading. J. Bone Miner. Res. 29 (5), 1118–1130.

Makowski, A.J., Patil, C.A., Mahadevan-Jansen, A., Nyman, J.S., 2013. Polarization control of Raman spectroscopy optimizes the assessment of bone tissue. J. Biomed. Opt. 18 (5), 55005.

McCreadie, B.R., Morris, M.D., Chen, T.C., Sudhaker Rao, D., Finney, W.F., Widjaja, E., Goldstein, S.A., 2006. Bone tissue compositional differences in women with and without osteoporotic fracture. Bone 39 (6), 1190–1195.

Mi, H., Muruganujan, A., Ebert, D., Huang, X., Thomas, P.D., 2019. PANTHER version 14: more genomes, a new PANTHER GO-slim and improvements in enrichment analysis tools. Nucleic Acids Res. 47 (D1), D419–D426.

Mirtz, T.A., Chandler, J.P., Eyers, C.M., 2011. The effects of physical activity on the epiphyseal growth plates: a review of the literature on normal physiology and clinical implications. J. Clin. Med. Res. 3 (1), 1–7.

Morey-Holton, E.R., Globus, R.K., 2002. Hindlimb unloading rodent model: technical aspects. J. Appl. Physiol. (1985) 92 (4), 1367–1377.

Morris, J.A., Kemp, J.P., Youlten, S.E., Laurent, L., Logan, J.G., Chai, R.C., Vulpescu, N. A., Forgetta, V., Kleinman, A., Mohanty, S.T., Sergio, C.M., Quinn, J., Nguyen-Yamamoto, L., Luco, A.L., Vijay, J., Simon, M.M., Pramatarova, A., Medina-Gomez, C., Trajanoska, K., Ghirardello, E.J., Butterfield, N.C., Curry, K.F., Leitch, V. D., Sparkes, P.C., Adoum, A.T., Mannan, N.S., Komla-Ebri, D.S.K., Pollard, A.S., Dewhurst, H.F., Hassall, T.A.D., Beltejar, M.G., , T. andMe Research, Adams, D.J., Vaillancourt, S.M., Kaptoge, S., Baldock, P., Cooper, C., Reeve, J., Ntzani, E.E., Evangelou, E., Ohlsson, C., Karasik, D., Rivadeneira, F., Kiel, D.P., Tobias, J.H., Gregson, C.L., Harvey, N.C., Grundberg, E., Goltzman, D., Adams, D.J., Lelliott, C.J., Hinds, D.A., Ackert-Bicknell, C.L., Hsu, Y.H., Maurano, M.T., Croucher, P.I., Williams, G.R., Bassett, J.H.D., Evans, D.M., Richards, J.B., 2019. An atlas of genetic influences on osteoporosis in humans and mice. Nat. Genet. 51 (2), 258–266.

Morse, A., Schindeler, A., McDonald, M.M., Kneissel, M., Kramer, I., Little, D.G., 2018. Sclerostin antibody augments the anabolic bone formation response in a mouse model of mechanical tibial loading. J. Bone Miner. Res. 33 (3), 486–498.

Newman, C.L., Moe, S.M., Chen, N.X., Hammond, M.A., Wallace, J.M., Nyman, J.S., Allen, M.R., 2014. Cortical bone mechanical properties are altered in an animal model of progressive chronic kidney disease. PLoS One 9 (6), e99262.

Oest, M.E., Gong, B., Esmonde-White, K., Mann, K.A., Zimmerman, N.D., Damron, T.A., Morris, M.D., 2016. Parathyroid hormone attenuates radiation-induced increases in collagen crosslink ratio at periosteal surfaces of mouse tibia. Bone 86, 91–97.

Patel, T.P., Gullotti, D.M., Hernandez, P., O'Brien, W.T., Capehart, B.P., Morrison 3rd, B., Bass, C., Eberwine, J.E., Abel, T., Meaney, D.F., 2014. An open-source toolbox for automated phenotyping of mice in behavioral tasks. Front. Behav. Neurosci. 8, 349.

Patterson-Buckendahl, P., Arnaud, S.B., Mechanic, G.L., Martin, R.B., Grindeland, R.E., Cann, C.E., 1987, 252 (2 Pt 2), R240–R246.

Peres-Ueno, M.J., Stringhetta-Garcia, C.T., Castoldi, R.C., Ozaki, G.A.T., Chaves-Neto, A. H., Dornelles, R.C.M., Louzada, M.J.Q., 2017. Model of hindlimb unloading in adult female rats: characterizing bone physicochemical, microstructural, and biomechanical properties. PLoS One 12 (12), e0189121.

Pertea, M., Pertea, G.M., Antonescu, C.M., Chang, T.C., Mendell, J.T., Salzberg, S.L., 2015. StringTie enables improved reconstruction of a transcriptome from RNA-seq reads. Nat. Biotechnol. 33 (3), 290–295.

Price, C., Herman, B.C., Lufkin, T., Goldman, H.M., Jepsen, K.J., 2005. Genetic variation in bone growth patterns defines adult mouse bone fragility. J. Bone Miner. Res. 20 (11), 1983–1991.

Robinson, M.D., McCarthy, D.J., Smyth, G.K., 2010. edgeR: a bioconductor package for differential expression analysis of digital gene expression data. Bioinformatics 26 (1), 139–140.

Sankaran, J.S., Varshney, M., Judex, S., 2017. Differences in bone structure and unloading-induced bone loss between C57BL/6N and C57BL/6J mice. Mamm. Genome 28 (11–12), 476–486.

Sibonga, J.D., Zhang, M., Evans, G.L., Westerlind, K.C., Cavolina, J.M., Morey-Holton, E., Turner, R.T., 2000. Effects of spaceflight and simulated weightlessness on longitudinal bone growth. Bone 27 (4), 535–540.

Simmons, D.J., Grynpas, M.D., Rosenberg, G.D., 1990. Maturation of bone and dentin matrices in rats flown on the soviet biosatellite cosmos 1887. FASEB J. 4 (1), 29–33.

Speacht, T.L., Krause, A.R., Steiner, J.L., Lang, C.H., Donahue, H.J., 2018. Combination of hindlimb suspension and immobilization by casting exaggerates sarcopenia by stimulating autophagy but does not worsen osteopenia. Bone 110, 29–37.

Svenson, K.L., Gatti, D.M., Valdar, W., Welsh, C.E., Cheng, R., Chesler, E.J., Palmer, A.A., McMillan, L., Churchill, G.A., 2012. High-resolution genetic mapping using the mouse diversity outbred population. Genetics 190 (2), 437–447.

Taylor, A.A.B., C, R., 1986. Bone strain: a determinant of gait and speed?.

Turner, C.H., Burr, D.B., 1993. Basic biomechanical measurements of bone: a tutorial. Bone 14 (4), 595–608.

Weaver, C.M., Gordon, C.M., Janz, K.F., Kalkwarf, H.J., Lappe, J.M., Lewis, R., O'Karma, M., Wallace, T.C., Zemel, B.S., 2016. The National Osteoporosis Foundation's position statement on peak bone mass development and lifestyle factors: a systematic review and implementation recommendations. Osteoporos. Int. 27 (4), 1281–1386.

Wergedal, J.E., Sheng, M.H.C., Ackert-Bicknell, C.L., Beamer, W.G., Baylink, D.J., 2005. Genetic variation in femur extrinsic strength in 29 different inbred strains of mice is dependent on variations in femur cross-sectional geometry and bone density. Bone 36 (1), 111–122.

Yerramshetty, J.S., Akkus, O., 2008. The associations between mineral crystallinity and the mechanical properties of human cortical bone. Bone 42 (3), 476–482.

Zhong, N., Garman, R.A., Squire, M.E., Donahue, L.R., Rubin, C.T., Hadjiargyrou, M., Judex, S., 2005. Gene expression patterns in bone after 4 days of hind-limb unloading in two inbred strains of mice. Aviat. Space Environ. Med. 76 (6), 530–535.